Direct electrochemical observation of glucosidase activity in isolated single lysosomes from a living cell

Rongrong Pan[a], Mingchen Xu[a], James D. Burgess[b], Dechen Jiang[a,1], and Hong-Yuan Chen[a]

[a]The State Key Laboratory of Analytical Chemistry for Life Science, School of Chemistry and Chemical Engineering, Nanjing University, 210093 Jiangsu, China; and [b]Department of Medical Laboratory, Imaging, and Radiologic Sciences, College of Allied Health Sciences, Augusta University, Augusta, GA 30912

Edited by Thomas E. Mallouk, The Pennsylvania State University, University Park, PA, and approved March 12, 2018 (received for review November 14, 2017)

The protein activity in individual intracellular compartments in single living cells must be analyzed to obtain an understanding of protein function at subcellular locations. The current methodology for probing activity is often not resolved to the level of an individual compartment, and the results provide an extent of reaction that is averaged from a group of compartments. To address this technological limitation, a single lysosome is sorted from a living cell via electrophoresis into a nanocapillary designed to electrochemically analyze internal solution. The activity of a protein specific to lysosomes, β-glucosidase, is determined by the electrochemical quantification of hydrogen peroxide generated from the reaction with its substrate and the associated enzymes preloaded in the nanocapillary. Sorting and assaying multiple lysosomes from the same cell shows the relative homogeneity of protein activity between different lysosomes, whereas the protein activity in single lysosomes from different cells of the same type is heterogeneous. Thus, this study for the analysis of protein activity within targeted cellular compartments allows direct study of protein function at subcellular resolution and provides unprecedented information about the homogeneity within the lysosomal population of a single cell.

subcellular analysis | electrochemical observation | single lysosomes | glucosidase activity | nanocapillary

Analyzing the localization, expression level, and reaction rates (e.g., activity) of proteins at the subcellular level is critical for an understanding of the amount of protein required to achieve its function and for better characterization of the effects of the local environment on reaction rates (1–3). Fast development of far-field superresolution fluorescence microscopy has circumvented the diffraction limit and visualized proteins in cellular compartments with a spatial resolution of less than 100 nm, thus allowing the determination of expression levels of proteins at the subcellular level (4–7). Building on these advancements in cellular analysis requires complementary technology where protein activity can be assessed without environmental perturbations imposed by fluorescence probes. With the considerable literature on various strategies to synthesize and implement novel probes for the optical investigation of protein localization within cells (8–11), the use of an electrochemical methodology to determine reaction rates in the absence of added species will allow refinements of conclusions from previous studies while also validating primary conclusions regarding subcellular features.

The current nanoelectrochemistry and corresponding theory are significantly improving detection limits and providing the feasibility of investigating local events in single cells with high spatiotemporal resolution. Recently established nanoelectrodes have been implemented to measure the amount of active neurotransmitters inside single vesicles and reactive oxygen/nitrogen species in individual phagolysosomes of living cells (12–16). For even greater function, nanopipettes are coated with carbon, gold, or platinum to fabricate multifunctional nanoring or nanopore electrodes in experiments for intracellular injections, electrical measurements, and electrophysiology (17–21). Single-molecule analysis is achieved by trapping and detection at the tip of a metallic nanopore (21).

In this work, an electrochemical detector is designed at the tip of a nanocapillary for isolation of a single entity of the desired compartment population and analysis of the protein activity in this compartment, such as β-glucosidase within a single lysosome. A capillary with a tip opening of ∼130 nm is coated with a platinum layer at the edge of the inner surface and the outer surface of the capillary (Fig. 1*A*). A silver wire coated with silver chloride (Ag/AgCl) is inserted into the capillary to be the reference electrode during the electrochemical measurement and to induce the electrophoresis of the cellular materials in the capillary tip (22, 23). This flux of cellular materials from outside to the inside of the capillary provides the ability to sort and isolate a target compartment by strategic placement of the capillary tip.

For protein reaction analysis and activity determination, the nanocapillary is withdrawn from the cell and held in air, thus creating a reaction chamber at the capillary tip that also serves as an electrochemical chamber for hydrogen peroxide oxidation in signal transduction. This small volume at the tip of the nanocapillary limits diffusion of the protein and hydrogen peroxide up into the capillary away from the desired reaction chamber, facilitating quantification of protein activity. Moreover, this experimental design only allows contact of the solution with the Pt layer inside the capillary so that an insulation material/process to cover Pt on the outer wall of the capillary is not required. After sorting and analysis of one lysosome, a positive voltage is applied on Ag/AgCl wire to reverse the flow direction of buffer, thus inducing egress of the previously loaded glucosidase and generated reaction debris. A series of sorting and detection experiments can thus be conducted at a single nanocapillary. That is, analysis of multiple compartments inside one cell can be characterized under the exact electrode/capillary geometry.

Significance

The quantification of protein activity in individual lysosomes in living cells is realized using a nanocapillary designed to electrochemically analyze internal solution, in which a single lysosome is sorted from the cell and the target protein is reacted with the corresponding kit components to generate hydrogen peroxide for measurement. The ability to sort and assay multiple lysosomes from the same cell allows direct study of protein function at subcellular resolution and provides unprecedented information about the homogeneity within the lysosomal population of a single cell.

Author contributions: D.J. and H.-Y.C. designed research; R.P. performed research; R.P., M.X., and D.J. analyzed data; and J.D.B. and D.J. wrote the paper.

The authors declare no conflict of interest.

This article is a PNAS Direct Submission.

[1]To whom correspondence should be addressed. Email: dechenjiang@nju.edu.cn.

This article contains supporting information online at www.pnas.org/lookup/suppl/doi:10.1073/pnas.1719844115/-/DCSupplemental.

Published online April 2, 2018.

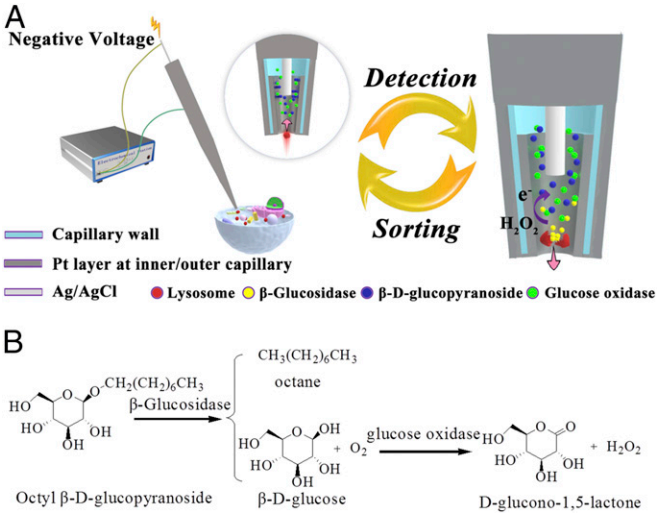

Fig. 1. (*A*) The scheme of electrochemical setup for the detection of glucosidase activity in isolated single lysosomes from a single cell. The capillary coated with a Pt layer (dark shading) and an Ag/AgCl wire (light shading) inserted in the capillary is connected with an electrochemical station. Circle: amplified view of capillary tip with a Pt layer at the edge of the inner surface and the outer surface of the capillary to sort one lysosome (labeled in red). The arrow exhibits the flow direction of buffer with the lysosome. Cross-section view is used to illustrate Pt layer at the inner capillary and kit reaction. (*Right*) Displaying the release of glucosidase after the lysis of lysosome, the generation of hydrogen peroxide from kit reactions and the following electrochemical detection of hydrogen peroxide at the tip (dark shading). The arrow exhibits the flow direction of previously loaded glucosidase and generated reaction debris outside the capillary. (*B*) Reaction process for the determination of glucosidase activity using β-D-glucopyranoside as the substrate and glucose oxidase as the coenzyme.

To demonstrate the analysis of protein activity in one cellular compartment, a single lysosome is chosen based on existing fluorescence labeling ability. The activity of β-glucosidase, a protein specific to lysosomes that is associated with Gaucher's disease, is analyzed using our nanocapillary with the embedded electrochemical function (24, 25). PBS (10 mM, pH 7.4) with β-D-glucopyranoside, glucose oxidase, and 1% Triton X-100 are the kit components placed in the nanocapillary for determination of glucosidase activity (Fig. 1*B*). After isolation of a single lysosome from the cytosol, Triton X-100 permeabilizes the lysosome membrane to release β-glucosidase, which hydrolyzes β-D-glucopyranoside to generate glucose. In the presence of glucose oxidase, glucose is oxidized to produce hydrogen peroxide for final signal transduction by electrochemical oxidation at the platinum electrode at the inner wall of the capillary tip. The amount of hydrogen peroxide generated over a specified reaction time provides information about the activity of β-glucosidase in one lysosome.

Results

Characterization of the Nanocapillary with the Electrochemical Detector. For the fabrication of the electrochemical detector inside the nanocapillary, the orifice of the capillary was faced toward the sputter source with an angle of 30° so that the Pt layer was deposited at the initial part of the inner capillary and the entire outer wall of the capillary (Fig. 2*A*). Different from our previous nanoring electrode that had only a ring of Pt layer at the tip and other nanoring electrodes (17–21, 23), the current electrode architecture had a Pt layer at the inner wall of the capillary to electrochemically detect hydrogen peroxide generated from the reaction with glucosidase.

The morphology of the orifice and Pt layer inside the capillary were characterized using SEM. The inner and outer diameters of the orifice from 14 capillaries were 132 ± 5 and 254 ± 5 nm, respectively (Fig. S1 *A* and *B*). The inclination of the tip (Fig. S1*B*) was measured to be 4.2° ± 0.6°. After focused ion beam (FIB) splitting along the tip, the Pt layer with a length of 6.5 ± 0.5 μm was observed (Fig. S1*C*) and was confirmed by energy dispersive spectroscopy (Fig. S1*D*). Adjusting the angle between the capillary and sputter source changed the length of the Pt layer inside the capillary. The angle of 90° introduced the Pt layer longer than 10 μm and the angle of 0° did not induce a Pt layer into the capillary. The angle of 30° is used in fabricating our electrodes for this work.

To characterize the active electrochemical area inside the capillary, the capillary was coupled with an Ag/AgCl wire and filled with 10 mM PBS (pH 7.4) containing 5 mM $[Fe(CN)_6]^{4-}$. After positioning the capillary in the air, cyclic voltammetry was performed (Fig. 2*B*). A near-steady-state current of 30 pA was observed, confirming the existence of a Pt layer inside the capillary as the active electrochemical surface and the feasibility of conducting electrochemical measurement with the capillary in air. A simulation of the voltammetry from this nanoband electrode using Comsol software is provided in Fig. S2 (26). Based on the simulated current, the length of the Pt layer inside the capillary was estimated to be ∼7 μm, which was consistent with the observation in SEM images.

Detection of Aqueous Glucosidase Activity. To validate the analysis of glucosidase activity using this nanocapillary with the electrochemical detector, the capillary filled with 5 mM β-D-glucopyranoside, 1 U/mL glucose oxidase, and 1% Triton X-100 was positioned above the solution. High concentrations of glucopyranoside and glucose oxidase are used to maximize the reaction rate and generate ample hydrogen peroxide. The optimization of reactant concentrations is provided in Fig. S3. A potential step of 600 mV was applied at the Pt electrode in the capillary using the Ag/AgCl wire inside the capillary as the reference electrode. After the background charge was collected (Fig. 3*A*, trace a), the capillary was immersed in the solution and the Ag/AgCl wire was connected with an Ag wire in the solution through an electrochemical station to induce the ingression of the solution with glucosidase into the capillary.

A voltage of −3 V was applied at the Ag/AgCl wire for 30 s to drive ∼1.75 fL of the solution containing glucosidase into the capillary (Fig. S4). The capillary was relocated to be held in air for 5 min to permit the conversion of glucopyranoside by glucosidase. This time also allowed solution on the outer capillary wall to dry, preventing electrochemistry at the external Pt. The small orifice of capillary restricted evaporation of water from inside the capillary and the solution volume in the capillary did not visibly change so that the concentrations of the kit components were not altered. A potential step of 600 mV was reapplied at the Pt electrode, and the charge traces corresponding to different glucosidase activities were collected (Fig. 3*A*, traces b–e).

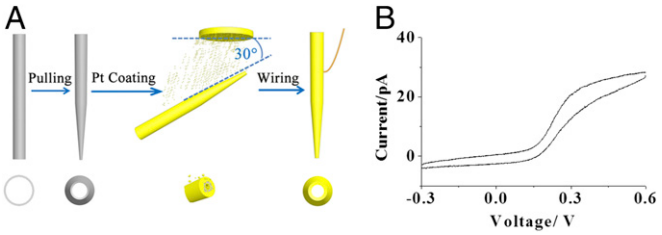

Fig. 2. (*A*) Fabrication of the nanoelectrode deposited with a Pt layer in the initial part of the inner capillary and at the entire outer wall of the capillary. (*B*) Cyclic voltammetry data of the nanoelectrode containing 10 mM PBS (pH 7.4) with 5 mM $[Fe(CN)_6]^{4-}$. The scan rate was 0.1 V/s.

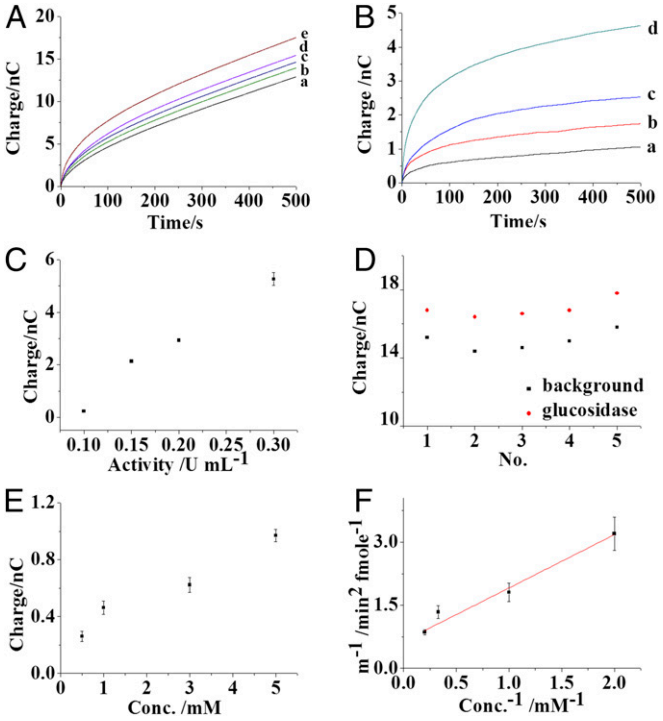

Fig. 3. (*A*) Charge traces of nanoelectrodes containing 10 mM PBS (pH 7.4) with 5 mM β-D-glucopyranoside, 1 U/mL glucose oxidase, 1% Triton X-100 (curve a), and 0.1 (curve b), 0.15 (curve c), 0.2 (curve d), and 0.3 (curve e) U/mL glucosidase. (*B*) Traces of the charge increase from the nanoelectrode before and after the loading of 0.1 (curve a), 0.15 (curve b), 0.2 (curve c), and 0.3 (curve d) U/mL glucosidase. (*C*) Correlation between the charge increase from the nanoelectrode and the protein activity. (*D*) Background charge and the charge before and after the loading of 0.15 U/mL glucosidase in five runs using one electrode. (*E*) The charge increase from the nanoelectrode at the first minute with different concentrations of β-D-glucopyranoside before and after the loading of 0.15 U/mL glucosidase. (*F*) Plot of 1/m and 1/conc. The value of m was the slope of $[H_2O_2]$ generated versus t^2 at the first minute, and conc. was the corresponding initial substrate (β-D-glucopyranoside) concentration. All of the measurements were performed under a potential of 600 mV in air. The error bar shows the SD calculated from four independent measurements.

After subtracting the background charge, the charge arising from the presence of glucosidase is clear (Fig. 3*B*, traces a–d). The increase in the charge reflects the amount of hydrogen peroxide generated from the enzyme reactions. Gradual increases in the charges are observed with higher glucosidase activity (Fig. 3*C*), demonstrating that our assay quantifies glucosidase activity.

During the 5-min holding time, glucosidase loaded into the capillary diffuses up the capillary and reacts with glucopyranoside to generate glucose and finally hydrogen peroxide that also diffuses in the capillary. The distributions of glucosidase and hydrogen peroxide in the capillary are modeled using Comsol software (*Supporting Information* and Fig. S5*A*). The tip orifice end of the capillary is a submicron channel (orifice: ∼130 nm, inclination: 4.2°, length 6 μm). The simulation result shows that glucosidase diffuses a distance of 1–3 μm from the tip orifice in this submicron channel (Fig. S5 *B* and *C*), as expected based on restricted diffusion of the protein in the nanochannel (27–29). The produced hydrogen peroxide diffuses faster and is thus more distributed in the capillary for the 5-min holding time (Fig. S5 *D* and *E*). It is noted that this estimation might have some error in describing the actual distribution of glucosidase and hydrogen peroxide, and more detailed experimentation is required to clarify this technical issue regarding diffusion.

Application of the 600-mV potential step at the Pt electrode results in a diffusional flux of hydrogen peroxide to the Pt electrode, while some hydrogen peroxide is lost to diffusion farther up the capillary. Thus, the rapid passage of charge at short time after the potential step and continuous passage of residual charge is consistent with the expected behavior for detection of hydrogen peroxide (Fig. 3*B*). Although a detailed description of the mass transfer phenomena inside the capillary is unavailable, three factors are clear. First, the inside of the capillary is tapered to form the tip where the Pt electrode is located and this feature allows a degree of nonlinear (partial radial) diffusion of hydrogen peroxide to the electrode from farther up in the capillary. Second, glucosidase is largely present at the front end of the capillary tip containing the Pt electrode and the kit components are at high concentrations such that associated substrate for enzymatic reactions is not depleted. Therefore, hydrogen peroxide generation is continuous during the potential step experiment. Finally, convective mass transport is very likely due to density fluctuations caused by the generation and accumulation of hydrogen peroxide before the potential step and the oxidative depletion of the hydrogen peroxide at the tip during the potential step (30). The produced convection inside the capillary serves to sustain the apparent limiting current that is measured for hydrogen peroxide electrooxidation. In this work, the electrochemical evaluation of hydrogen peroxide in the capillary allows calculation of the average rate of hydrogen peroxide generation during the reaction time and potential step experiment, and thus reports the overall reaction rate that is dependent on glucosidase activity.

Control experiments were conducted by the exclusion of either glucopyranoside or glucose oxidase from the capillary so that there was no generation of hydrogen peroxide from glucopyranoside. No charge increase was observed after loading of glucosidase (Fig. S6 *A* and *B*). These results confirmed that the higher level of charge observed is from the conversion of glucopyranoside in the presence of glucosidase. The charge for different loading conditions was investigated by varying the applied voltage and time. More charge is observed with a higher voltage and longer loading time (Fig. S6 *C* and *D*). This result reflected increased glucosidase loaded into the capillary.

A thin aqueous film on a portion of the hydrophilic Pt-coated outer surface of the capillary adjacent to the orifice might exist, and thus the reaction of glucosidase in this film could contribute to the total charge. To investigate this possibility, a control experiment was performed by dipping the capillary in 0.2 U/mL glucosidase solution. No voltage was applied at Ag/AgCl wire so that no solution with glucosidase was loaded into the capillary, but rather only introduced into the thin film outside the tip. Compared with the background charge, no charge increase was observed, suggesting an insignificant contribution from this possibility (Fig. S6 *E* and *F*).

The reactions occur at the tip of capillary and only a small amount of the substrate is consumed in the capillary. Thus, the concentrations of substrate were modeled as being constant during the measurement. The relative SDs of four independent measurements using different nanoelectrodes were less than 12.1%, establishing the reproducibility of the assay. Compared with the immobilization of glucopyranoside and glucose oxidase on the Pt electrode inside the capillary, the use of solution resident kit components better maintains repeatable enzymatic activity as fresh material is loaded for each run (31).

To compare the protein activity in different lysosomes from one cell, continuous sorting and analysis of multiple single lysosomes from the same cell were conducted using the same nanocapillary. The debris from the previous lysosome experiment, including glucosidase, was removed from the capillary so that the next process could be performed with fresh reactants. The technical means of achieving solution exchange was the application of 3 V at the Ag/AgCl wire for 30 s to remove the solution in the reaction region from the capillary. Typically, the background charge dropped to the initial value (Fig. 3*D*), suggesting the successful

exclusion of glucosidase from the capillary and the introduction of fresh solution. The charge increase from these five replicate loadings of 0.15 U/mL glucosidase into the capillary exhibited a relative SD of 9.52%, which revealed the feasibility of reproducibly analyzing multiple lysosomes in one cell using one nanoelectrode. After more than about five measurements, however, an obvious increase in the background charge is observed, likely indicating the possible adsorption of proteins at the Pt electrode or the alternation of the Pt surface structure. Therefore, five measurements are the limit of the nanoelectrode's lifetime.

The determination of K_m provides kinetic information about the interaction between the substrate and the enzyme, which is important for evaluating protein activity. In the capillary, the concentration of glucopyranoside is varied and the corresponding reaction rates are recorded to evaluate the Michaelis constant (K_m) (Fig. 3*E*). The detail for the evaluation of K_m is shown in *Determination of Michaelis Constant of Glucosidase*. Since the initial charge increase is predominantly from hydrogen peroxide generated during the 5-min reaction time (also drying time), the derivation of charge increase over time squared (t^2) at 1 min during the potential step experiment is used to estimate the initial slope of $[H_2O_2]$ versus t^2 (more description in experimental section) so that the approximate relationship between 1/m and 1/C (concentration) is obtained (Fig. 3*F*). After linear fitting ($R^2 = 0.90$) and the determination of the intercept on the abscissa, the K_m value of glucosidase for glucopyranoside is estimated to be 1.67 mM, which is close to the literature value (32). These results support the notion that our electrochemical detector system can provide the activity of and approximate kinetic information for proteins.

Sorting One Lysosome into the Nanocapillary with the Electrochemical Detector. The analysis of glucosidase activity in single lysosomes is performed on cells that were labeled with a fluorescent lysosome marker, LysoTracker, to visualize the lysosomes. Before sorting of a single lysosome, the background charge from the electrochemical detector is collected in air (Fig. S7*A*, curve a). Then, the capillary is inserted into the cell, and the position of the capillary tip is adjusted inside the cell to reach the region with multiple single lysosomes as observed under fluorescence microscopy (Fig. 4 *A*–*C*). Previous literature reports demonstrate that single lysosomes in living cells are observed to have sizes of ~300 and ~100 nm under conventional and superresolution fluorescence imaging, respectively. Therefore, the fluorescence spots of 300~400 nm observed in the fluorescence image (Fig. 4*C*, *Inset*) are assigned to a single lysosome. Care is taken to include data for isolation of a matched lysosome aliquot as gauged by the size of the fluorescence image representing the lysosome fraction that is captured. Due to the movement of lysosomes in living cells, the sorting process is initiated immediately after the fluorescence visualization to avoid losing the target lysosome.

Experimentally, a voltage of −3 V is applied at the Ag/AgCl wire inside the capillary for 30 s until one lysosome (pointed to in Fig. 4*C*, *Inset*) near the capillary tip disappears from the fluorescence image (Fig. 4*D*). Adjacent lysosomes that were 1~2 μm away from the target lysosome remained and did not move significantly. This is strong evidence for our ability to isolate a target lysosome. The success rate of sorting one fluorescence spot/lysosome is about 40% and in other cases no lysosome is loaded or more than one lysosome is loaded into the capillary.

The current flowing through the metal wire inside the capillary drops by one-half upon the position of the capillary inside the cell (Fig. S7*C*). This suggests a doubling of the resistance with the plasma membrane resistance being comparable to the capillary resistance. With the voltage applied at the metal wire in the capillary, the produced electric field reflects the voltage drop caused by the capillary and plasma membrane resistance. Under this electric field, both electrophoresis and electroosmosis flow might be involved to induce the transport of lysosome into the capillary. To investigate the loading process, the physiological PBS concentration in the capillary was elevated to 50 mM (500 mM NaCl included), which increased the ionic strength of the solution and resulted in a decrease of electroosmotic flow inside the capillary. No significant interruption in the loading of single lysosomes was observed, which suggested that the transport of lysosomes was most likely via electrophoresis. The electroosmosis flow that assists the migration of the lysosome through the flow of cytosol might still exist. When the voltage was removed from the metal wire, no disappearance of lysosome near the capillary orifice indicated the minor contribution of random motion of lysosome.

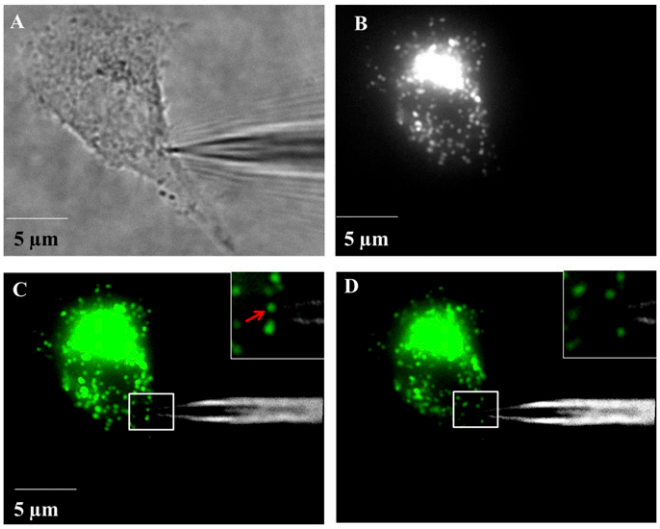

Fig. 4. (*A*) Bright-field image of the insertion of a nanoelectrode into a living HeLa cell. (*B*) Fluorescence image of the living cell stained with LysoTracker for the visualization of lysosomes. (*C*) Overlapping of image *A* and *B*. (*D*) Overlapping image of the nanoelectrode and the cell immediately after the sorting of one lysosome into the capillary. The insets in image *C* and *D* are the amplified display of the rectangular region in image *C* and *D*. The fluorescence at the lysosomes was false-colored into green for better visualization. The fluorescence spot arrowed in image *C* (*Inset*) was the lysosome sorted.

Analysis of Glucosidase Activity in One Lysosome. After successful loading of a single target lysosome into the capillary, the capillary is relocated into air for 5 min. During this time, the lysosome is lysed immediately by Triton X-100 to release glucosidase, other proteins, and lipids near the orifice. Similar to the previous estimation regarding diffusion of glucosidase in the capillary, most of glucosidase released should be located at the Pt electrode region. The charge is collected after the reaction time (Fig. S7*A*, curve b) and the increase in charge reflects the introduction of glucosidase. Since glucosidase is a specific protein in lysosomes, these data indicated the successful sorting and the detection of glucosidase activity in the lysosome (Fig. 5*A*, trace a).

Triton X-100 is a critical component in our assay as it is required for the permeabilization of the lysosome membrane to release glucosidase. A control experiment was performed without Triton X-100 in the capillary and no charge increase was observed for the introduction of a single lysosome into the capillary (Fig. 5*A*, trace b and Fig. S7 *B* and *D*). This result showed that the release of glucosidase from the lysosome is required for the assay of the glucosidase activity. Also, as discussed above, a thin aqueous layer including Triton X-100 is expected to exist on the outer wall near the orifice. This solution could be introduced into the cell during the insertion of the capillary and cause altered cellular activity. Therefore, the intracellular Ca ion

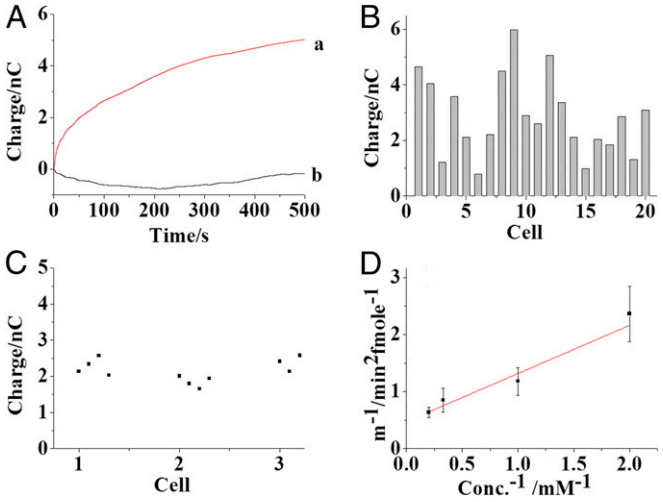

Fig. 5. (*A*) Traces of the charge increase from the nanoelectrode containing 10 mM PBS (pH 7.4) with 5 mM β-D-glucopyranoside, 1 U/mL glucose oxidase, and 1% Triton X-100 before and after the loading of one lysosome into the capillary (trace a). Trace b represents the charge difference before and after the loading of one lysosome into the capillary in the absence of Triton X-100. (*B*) Charge increases from the nanoelectrode after the sorting of single lysosomes in 20 individual cells. Each column presents one charge measurement from one lysosome in one individual cell. (*C*) Charge increase from four individual lysosomes in three cells, numbered as 1, 2, and 3. (*D*) Plot of 1/m and 1/conc. All of the measurements were performed under a potential of 0.6 V in air. The error bar presents the SD calculated from three independent measurements.

concentration was evaluated using Fluo-3 as a fluorescence probe before and after the capillary insertion. No change of fluorescence intensity was observed (Fig. S8*A*) for the insertion of the capillary, suggesting insignificant influence of introduced Triton X-100 on cellular activity.

During the sorting of an individual lysosome, some cytosol might be loaded into the capillary as well. The components in the cytosol, except intracellular glucose, would not react with either glucopyranoside or glucose oxidase to generate hydrogen peroxide. Since intracellular glucose loaded into the capillary would generate additional hydrogen peroxide, another control experiment was performed for the removal of glucopyranoside from the capillary. No charge increase for the addition of glucose during lysosome isolation is observed, suggesting that intracellular glucose entering the capillary is negligible. The concentration of glucose in cells is 1–5 mM (33). For example, 1.75 fL cytosol containing a maximal 0.009 fmol of glucose loaded into the capillary would generate a charge of 1.8 pC and this charge is negligible relative to the signal. To further support the analysis of protein activity in a single lysosome, the capillary is inserted into the nucleus of cells where no glucosidase exists. The analysis showed no charge increase (Fig. S7*D*). Overall, these control experiments strongly support the conclusion that analysis of a single lysosome is achieved.

The glucosidase activities in single lysosomes from 20 individual HeLa cells were investigated as summarized in Fig. 5*B*. The charge increase is 2.86 ± 1.43 nC. Based on the calibration curve in Fig. 3*C*, this charge increase reflects an average activity of 35 pU for glucosidase in one lysosome. The relative SD (RSD) of this analysis from the 20 cells is 50.0%, which is much larger than the electrode–electrode difference (RSD 12.1%) characterized from aqueous solution experiments. Therefore, similar to other results from single-cell analysis (34, 35), a high cellular heterogeneity of glucosidase activity is observed.

Importantly, the characterization of glucosidase activity in four lysosomes (300~400 nm) isolated from one cell using the same nanoelectrode exhibited a much smaller RSD (Fig. 5*C*; RSD 10.4%, 8.3%, and 8.13% from three individual cells), which is similar to the systematic measurement error (RSD 9.52%) characterized for the nanoelectrodes from aqueous solution data. This surprising observation of similar charge increase for comparably sized lysosomes argues for a degree of homogeneity of glucosidase activity in different lysosomes within the same cell. This evidence suggests that cellular heterogeneity of glucosidase activity might originate from the complex interaction of glucosidase or lysosomes with other components in the cell. Indirectly, this result suggests that different lysosomes from one cell have a similar cellular environment, as it is highly unlikely that different amounts of glucosidase would be regulated to a similar activity through matrix effects. Since cell-to-cell variation arises in part from the inherent variability that can be intrinsic or extrinsic, elucidating the biochemical origins of cellular heterogeneity could help in the understanding of biological mechanisms and ultimately in the diagnosis and treatment of cancer.

Due to this homogeneity of glucosidase in the individual lysosomes from one cell, the slightly larger fluorescence spot (600~800 nm) corresponding to a lysosome cluster with two compartments in the same cells was analyzed. Compared with similar charge increases from the apparent single lysosomes, a 2.03 ± 0.3-fold increase in charge is recorded from large spots (Fig. S8*B*). The correlation of charge increase and the lysosome number in one spot supports that our strategy could sort and analyze glucosidase activity in single lysosomes based on the spot size in fluorescence imaging.

Moreover, single lysosomes were individually sorted into the capillaries with different concentrations of glucopyranoside to estimate the K_m of glucosidase in the lysosomes. For statistics, three cells with similar glucosidase activity were selected for the electrochemical measurement. Although the cell–cell and lysosome–lysosome differences were controlled, it was noted that a significant systematic error might exist in our measurement of the K_m value of glucosidase in the lysosomes. Despite this challenge, our measurements provided direct, approximate, kinetic information about protein function in a particular intracellular compartment. The K_m of glucosidase in the lysosome was estimated to be ~1.79 mM (Fig. 5*D*). For comparison, a population of 10^6 cells was lysed, and the cytosol with glucosidase was isolated. Femtoliter cytosol aliquots were loaded into the capillary, and the K_m value of glucosidase from the cell population was determined to be ~0.52 mM (Fig. S8*C*). Compared with the value from the cell lysate, the K_m value for the single cell/lysosome experiments was closer to that of pure protein, suggesting complications in the cell lysate measurement due to the presence of cellular debris. The approximate measurement of the K_m value of the protein in the lysosome offers a special strategy for evaluating protein activity at the subcellular level, which might provide new insight into protein function in cellular compartments.

Conclusion

Protein activity in a single cellular compartment, such as lysosomes, is achieved using a nanocapillary with the electrochemical detector. The ability to sort and measure multiple single lysosomes continuously in one living cell permits the evaluation of protein homogeneity at the subcellular level. The observation of similar protein activities in different lysosomes in one cell suggests the relative uniformity of the subcellular environment, indicating a standardization of the protein activity in the compartments. However, one living cell as a functional and complex system might have many variations inside that lead to differences in the subcellular environment and the protein distribution relative to other cells. Indeed, a high heterogeneity of protein activity in different cells of the same type is observed as well. A thorough investigation must be performed to elucidate this cellular heterogeneity and subcellular homogeneity and, ultimately, to facilitate a deeper understanding of cellular function.

Methods

Fabrication of the Nanocapillary with the Electrochemical Detector. A glass capillary (BF100-58-10) was pulled using a micropipette puller (P2000; Sutter Instrument Co.) to create a tip with a ~130-nm opening. The capillary was positioned to face a Pt sputter source during sputtering for 8 min so that the Pt layer was deposited in the initial part of the inner capillary as the electrochemical detector. Then, the whole outer wall of the capillary was continuously sputtered to produce a Pt layer with a thickness of ~70 nm. A copper wire was attached at Pt layer on the outer wall of the capillary for the connection of the capillary with electrochemical station. The capillary tips covered with a Pt layer were characterized using SEM (Hitachi S-4800 Instrument) with an accelerating voltage of 10 kV.

Electrochemical Measurement. The Pt layer at the outer wall of capillary was connected with an electrochemical station (CHI 630E; CH Instruments) as the working electrode. The Pt layer inside the capillary was designed as the electrochemical-active region for the detection of hydrogen peroxide produced from the kit reaction. One Ag/AgCl wire was placed inside the capillary and one Ag wire was positioned in the buffer. To initiate the flow toward the capillary orifice, the capillary was positioned in the buffer and a voltage was applied between the Ag/AgCl wire inside the capillary and the Ag wire in the buffer for the loading of solution or lysosome into the capillary. Immediately after the loading process, the capillary was repositioned in the air for 5 min, and a voltage of 600 mV was introduced between the working electrode and Ag/AgCl wire inside the capillary for electrochemical measurement.

Detection of Aqueous Glucosidase Activity. For the detection of glucosidase activity, the kit components, including 10 mM PBS (pH 7.4) with 5 mM β-D-glucopyranoside, 1 U/mL glucose oxidase, and 1% Triton X-100, were filled into the capillary. Initially, the capillary with the kit components was positioned in the air and a voltage of 600 mV was applied at the Pt layer on the capillary to record the nonfaradic charge as the background charge (recording). Only the capillaries with similar background charge were used for the analysis. Then, the capillary was immersed into the buffer to complete the electrochemical loading (loading). Later, the capillary was repositioned in the air and the voltage of 600 mV was applied again to collect additional charge from the kit reaction (measurement).

After completing a recording–loading–measurement procedure, a positive voltage of 3 V was applied between the Ag/AgCl wire inside the capillary and the Ag wire in the buffer to remove the loaded components and the reaction debris from the capillary. The same recording–loading–measurement procedure was repeated for serial analysis.

Fluorescence Visualization of Lysosomes Inside the Cell. The living cells attached to a Petri dish were treated with 10 mM PBS containing 100 nM LysoTracker Red DND-99 (excitation/emission 577/590 nm) for 1 h at 37 °C. After washing and cultured in fresh PBS, the cells were imaged using fluorescence microscopy (Olympus X51). The exposure time was set as 1 s.

Analysis of Glucosidase Activity in Single Lysosomes. The capillary with the kit components was mounted on a 3D translation stage and held in the air to collect background charge. Then, the capillary was inserted into the cell under fluorescence microscopy and positioned in the region where single lysosomes were distinguished. With the capillary tip near one lysosome, the fluorescence image was recorded. Immediately after imaging, the voltage of −3 V was applied between the Ag/AgCl wire inside the capillary and the Ag wire in the buffer for 30 s to sort the target lysosome. The fluorescence image was retaken to confirm the disappearance of this lysosome. After the sorting of this lysosome, the electrode was repositioned in the air for 5 min following the electrochemical measurement of hydrogen peroxide generated from kit reactions.

ACKNOWLEDGMENTS. We thank Dr. Zeng-qiang Wu for the guidance in the simulation. This work was supported by National Natural Science Foundation of China Grants 21327902 and 21575060 and Ministry of Science and Technology of China Grant 2016YFA0201203.

1. Altschuler SJ, Wu LF (2010) Cellular heterogeneity: do differences make a difference? *Cell* 141:559–563.
2. Larance M, Lamond AI (2015) Multidimensional proteomics for cell biology. *Nat Rev Mol Cell Biol* 16:269–280.
3. Yates JR, 3rd, Gilchrist A, Howell KE, Bergeron JJM (2005) Proteomics of organelles and large cellular structures. *Nat Rev Mol Cell Biol* 6:702–714.
4. Huang B, Bates M, Zhuang X (2009) Super-resolution fluorescence microscopy. *Annu Rev Biochem* 78:993–1016.
5. Betzig E, et al. (2006) Imaging intracellular fluorescent proteins at nanometer resolution. *Science* 313:1642–1645.
6. Rust MJ, Bates M, Zhuang X (2006) Sub-diffraction-limit imaging by stochastic optical reconstruction microscopy (STORM). *Nat Methods* 3:793–795.
7. Klar TA, Hell SW (1999) Subdiffraction resolution in far-field fluorescence microscopy. *Opt Lett* 24:954–956.
8. Wachsmuth M, et al. (2015) High-throughput fluorescence correlation spectroscopy enables analysis of proteome dynamics in living cells. *Nat Biotechnol* 33:384–389.
9. Wang C, Han B, Zhou R, Zhuang X (2016) Real-time imaging of translation on single mRNA transcripts in live cells. *Cell* 165:990–1001.
10. Barbe L, et al. (2008) Toward a confocal subcellular atlas of the human proteome. *Mol Cell Proteomics* 7:499–508.
11. Stadler C, et al. (2013) Immunofluorescence and fluorescent-protein tagging show high correlation for protein localization in mammalian cells. *Nat Methods* 10: 315–323.
12. Phan NTN, Li XC, Ewing AG (2017) Measuring synaptic vesicles using cellular electrochemistry and nanoscale molecular imaging. *Nat Rev Chem* 1:0048.
13. Li X, Majdi S, Dunevall J, Fathali H, Ewing AG (2015) Quantitative measurement of transmitters in individual vesicles in the cytoplasm of single cells with nanotip electrodes. *Angew Chem Int Ed Engl* 54:11978–11982.
14. Dunevall J, et al. (2015) Characterizing the catecholamine content of single mammalian vesicles by collision-adsorption events at an electrode. *J Am Chem Soc* 137: 4344–4346.
15. Zhang XW, et al. (2017) Real-time intracellular measurements of ROS and RNS in living cells with single core-shell nanowire electrodes. *Angew Chem Int Ed Engl* 56: 12997–13000.
16. Li Y, et al. (2017) Direct electrochemical measurements of reactive oxygen and nitrogen species in nontransformed and metastatic human breast cells. *J Am Chem Soc* 139:13055–13062.
17. Pérez-Mitta G, Marmisollé WA, Trautmann C, Toimil-Molares ME, Azzaroni O (2015) Nanofluidic diodes with dynamic rectification properties stemming from reversible electrochemical conversions in conducting polymers. *J Am Chem Soc* 137:15382–15385.
18. Singhal R, et al. (2010) Small diameter carbon nanopipettes. *Nanotechnology* 21: 015304.
19. Hu K, et al. (2014) Open carbon nanopipettes as resistive-pulse sensors, rectification sensors, and electrochemical nanoprobes. *Anal Chem* 86:8897–8901.
20. Yang C, Hinkle P, Menestrina J, Vlassiouk IV, Siwy ZS (2016) Polarization of gold in nanopores leads to ion current rectification. *J Phys Chem Lett* 7:4152–4159.
21. Freedman KJ, et al. (2016) Nanopore sensing at ultra-low concentrations using single-molecule dielectrophoretic trapping. *Nat Commun* 7:10217.
22. Laforge FO, Carpino J, Rotenberg SA, Mirkin MV (2007) Electrochemical attosyringe. *Proc Natl Acad Sci USA* 104:11895–11900.
23. Pan R, Xu M, Jiang D, Burgess JD, Chen HY (2016) Nanokit for single-cell electrochemical analyses. *Proc Natl Acad Sci USA* 113:11436–11440.
24. Fabbro D, Desnick RJ, Gatt S (1984) Lysosomal beta-glucosidase of rat liver. *Enzyme* 31:122–127.
25. Steet RA, et al. (2006) The iminosugar isofagomine increases the activity of N370S mutant acid beta-glucosidase in Gaucher fibroblasts by several mechanisms. *Proc Natl Acad Sci USA* 103:13813–13818.
26. Zhang B, Zhang Y, White HS (2006) Steady-state voltammetric response of the nanopore electrode. *Anal Chem* 78:477–483.
27. Durand NFY, Bertsch A, Todorova M, Renaud P (2007) Direct measurement of effective diffusion coefficients in nanochannels using steady-state dispersion effects. *Appl Phys Lett* 91:203106.
28. Pappaert K, Biesemans J, Clicq D, Vankrunkelsven S, Desmet G (2005) Measurements of diffusion coefficients in 1-D micro- and nanochannels using shear-driven flows. *Lab Chip* 5:1104–1110.
29. Streletzky K, Phillies GD (1995) Temperature dependence of triton X-100 micelle size and hydration. *Langmuir* 11:42–47.
30. Pebay C, Sella C, Thouin L, Amatore C (2013) Mass transport at infinite regular arrays of microband electrodes submitted to natural convection: theory and experiments. *Anal Chem* 85:12062–12069.
31. Xu H, Zhou S, Jiang D, Chen HY (2018) Cholesterol oxidase/triton X-100 parked microelectrodes for the detection of cholesterol in plasma membrane at single cells. *Anal Chem* 90:1054–1058.
32. Dale MP, Kopfler WP, Chait I, Byers LD (1986) Beta-glucosidase: substrate, solvent, and viscosity variation as probes of the rate-limiting steps. *Biochemistry* 25:2522–2529.
33. Nascimento RA, et al. (2016) Single cell "glucose nanosensor" verifies elevated glucose levels in individual cancer cells. *Nano Lett* 16:1194–1200.
34. Meredith GD, Sims CE, Soughayer JS, Allbritton NL (2000) Measurement of kinase activation in single mammalian cells. *Nat Biotechnol* 18:309–312.
35. Zhang B, et al. (2008) Spatially and temporally resolved single-cell exocytosis utilizing individually addressable carbon microelectrode arrays. *Anal Chem* 80:1394–1400.